Earth Surf. Dynam. Discuss., 1, 1097–1126, 2013
www.earth-surf-dynam-discuss.net/1/1097/2013/
doi:10.5194/esurfd-1-1097-2013

Earth Surface Dynamics Discussions
Open Access

Morphodynamics of river bed variation with variable bedload step length

A. Pelosi[1] and G. Parker[2]

[1]Department of Civil Engineering, Università degli Studi di Salerno (UNISA), Salerno, Italy
[2]Department of Civil & Environmental Engineering and Department of Geology, Hydrosystems Laboratory, University of Illinois, 301 N. Mathews Ave., Urbana, IL 61801, USA

Received: 25 October 2013 – Accepted: 31 October 2013 – Published: 22 November 2013

Correspondence to: A. Pelosi (apelosi@unisa.it)

Published by Copernicus Publications on behalf of the European Geosciences Union.

Abstract

Here we consider the 1-D morphodynamics of an erodible bed subject to bedload transport. Fluvial bed elevation variation is typically modeled by the Exner equation which, in its classical form, expresses mass conservation in terms of the divergence of the bedload sediment flux. An entrainment form of the Exner equation can be written as an alternative description of the same bedload processes, by introducing the notions of an entrainment rate into bedload and of a particle step length, and assuming a certain probability distribution for the step length. This entrainment form implies some degree of non-locality which is absent from the standard flux form, so that these two expressions, which are different ways to look at same conservation principle (i.e. sediment continuity), may no longer become equivalent in cases when channel complexity and flow conditions allow for long particle saltation steps (including, but not limited to the case where particle step length has a heavy tailed distribution) or when the domain of interest is not long compared to the step length (e.g. laboratory scales, or saltation over relatively smooth surfaces). We perform a systematic analysis of the effects of the non-locality in the entrainment form of Exner equation on transient aggradational/degradational bed profiles by using the flux form as a benchmark. As expected, the two forms converge to the same results as the step length converges to zero, in which case non-locality is negligible. As step length increases relative to domain length, the mode of aggradation changes from an upward-concave form to a rotational, and then eventually a downward-concave form. Corresponding behavior is found for the case of degradation. These results may explain anomalously flat aggradational long profiles that have been observed in some short laboratory flume experiments.

1 Introduction

The Exner equation of sediment conservation, when combined with a hydrodynamic model and a sediment transport model, is a central tool to evaluate the bed evolu-

ESURFD

1, 1097–1126, 2013

tion (e.g. aggradation and degradation) in the field of morphodynamics of the Earth's surface.

The Exner equation, in its classical formulation, relates the bed evolution to the divergence of the bedload sediment flux (q), which is assumed to be a local function of the flow and the topography. However, certain sediment dynamics, such as (i) particle diffusion in river bedload (e.g. Nikora et al., 2002; Bradley et al., 2010; Ganti et al., 2010; Martin et al., 2012), (ii) bed sediment transport along bedrock channels (Stark et al., 2009) and (iii) particle displacements on hillslopes (Foufoula-Georgiou et al., 2010) may show non-local behaviour that is not easily captured by the classical form of the Exner equation.

The non-locality of interest here is embedded in the step length r of a bedload particle, i.e. the distance that a particle, once entrained into motion, travels before depositing. The existence of a finite step length r implies a non-local connection between point x (where a particle is deposited) and point x–r (where it was entrained). The degree of non-locality can be characterized in terms of the probability density (pdf) of step lengths $f_s(r)$. This pdf can be hypothesized to be thin-tailed (e.g. exponential) or heavy-tailed (e.g. power).

In recent years, considerable emphasis has been placed on non-locality associated with heavy-tailed pdf's for step length (e.g. Schumer et al., 2009; Bradley et al., 2010; Ganti et al., 2010). This appears to be in part motivated by the desire to construct fractional advective-diffusive equations for pebble tracer dispersion corresponding to the now-classical fADE model (e.g. Schumer et al., 2009).

Experiments conducted under the simplest possible conditions (including steady, uniform flow, single-sized sediment and the absence of bedforms) yield thin-tailed, and more specifically exponential distributions for step length pdf (Nakagawa and Tsujimoto, 1980; Hill et al., 2010). Ganti et al. (2010), however showed that were (a) the bed to consist of a range of sizes, (b) the pdf of size distribution to obey a gamma distribution and (c) the pdf of for step length of each grain size to be exponential, the resulting pdf for step length would be heavy-tailed. Hassan et al. (2013) analysed 64 sets of field

ESURFD
1, 1097–1126, 2013

data on pebble tracer dispersion in mountain rivers (which by nature contain a range of sizes). They found that all but 5 cases either showed thin-tailed pdf's, or could be rescaled as thin-tailed pdf's. Their results, combined with those of Ganti et al. (2010), however, do suggest that the gradual incorporation of the many factors in nature that lead to complexity can also lead to non-local behaviour mediated by heavy-tailed pdf's.

Here, however, we focus on the case of non-locality mediated by thin-tailed (exponential) pdf's for step length. Regardless of the thin tail of the pdf, the degree of non-locality nevertheless increases with increasing mean step length $\bar{r}$. This non-locality may become dominant when $\bar{r}$ approaches the same order of magnitude as the domain length L_d under consideration. We show that patterns of bed aggradation and degradation are strongly dependent on the ratio $\bar{r}/L_d$, a parameter that may be surprisingly large in some small-scale experiments. Our results may explain anomalously flat aggradational long profiles that have been observed in some short laboratory flume experiments, without relying on either of the fractional partial differential equations or heavy-tailed distributions invoked or implied by Voller and Paola (2010). We use our framework to explore the consequences of heavy-tailed pdf's for step lengths as well.

2 Methods

2.1 Theoretical framework

1-D river bed elevation variation is classically described by the 1-D Exner equation of sediment conservation in flux form (or equivalently in the 2-D case, divergence form):

$$\frac{\partial \eta(x,t)}{\partial t} = -\frac{\partial q(x,t)}{\partial x} \tag{1}$$

where η [L] denotes the bed elevation, t [T] denotes the time, x [L] denotes the streamwise distance and q [L^2T^{-1}] is the volume bedload transport rate per unit width. (Here, the porosity of the bed sediment is set = 0 and bedload only is considered, both for

ESURFD
1, 1097–1126, 2013

A. Pelosi and G. Parker

the sake of simplicity.) There is, however, a completely equivalent entrainment form of sediment conservation (e.g. Tsujimoto, 1978):

$$\frac{\partial \eta(x,t)}{\partial t} = D(x,t) - E(x,t) \tag{2}$$

where E [LT^{-1}] denotes the volume rate of entrainment of bed particles into bedload per unit area per unit time and D [LT^{-1}] denotes the volume rate of deposition of bedload material onto the bed per unit area per unit time.

The deposition rate can be related to the entrainment rate by means of the probability density of the step length $f_s(r)$ [L^{-1}], that is the probability density of the distance that an entrained particle moves before being re-deposited. Assuming that, once entrained, a particle undergoes a step with length r before depositing, and that this step length has the probability density $f_s(r)$ (pdf of step length), the volume deposition rate D can be specified as follows in terms of entrainment rate upstream and travel distance (e.g. Parker et al., 2000; Ganti et al., 2010),

$$D(x) = \int_0^\infty E(x-r) f_s(r) \mathrm{d}r \tag{3}$$

so that the entrainment form of sediment mass conservation can be written as:

$$\frac{\partial \eta}{\partial t} = -E(x) + \int_0^\infty E(x-r) f_s(r) \mathrm{d}r \tag{4}$$

As has been shown by Tsujimoto (1998), the two forms Eqs. (1) and (4), are in principle completely equivalent in so far as the following equation precisely describes the bedload transport rate:

$$q(x) = \int_0^\infty E(x-r) \int_r^\infty f_s(r') \mathrm{d}r' \mathrm{d}r \tag{5}$$

Discussion Paper | Discussion Paper | Discussion Paper | Discussion Paper |

ESURFD

1, 1097–1126, 2013

Morphodynamics of river bed variation with variable bedload step length

A. Pelosi and G. Parker

Yet in any given implementation, they are rarely equivalent. More specifically, in most implementations of the flux form Eq. (1), q is taken to be a local function of the flow (e.g. bed shear stress), whereas in most implementations of the entrainment form Eq. (4), E is taken to be a local function of the flow (again, e.g. bed shear stress). The presence of the spatial convolution term in the entrainment form of Eqs. (3) and (4) ensures non-locality in the entrainment form as compared to the flux form. This non-locality is present regardless of whether the pdf of step length $f_s(r)$ is thin-tailed or heavy-tailed, and vanishes only when $f_s(r)$ becomes proportional to $\delta(r)$, where δ denotes the Dirac function.

Here we explore the consequences of non-locality, and compare the local and non-local forms Eqs. (1) and (4) for Exner over a range of conditions. To do this, we assume that the pdf $f_s(r)$ has a mean step length, and consider the dimensionless parameter ε:

$$\varepsilon = \frac{\overline{r}}{L_\mathrm{d}} \tag{6}$$

where $\overline{r}$ [L] denotes the mean particle step length and L_d [L] denotes the length of the domain of interest (e.g. flume length or length of river reach). The flux and entrainment forms become strictly equivalent only under the constraint:

$$\varepsilon = \frac{\overline{r}}{L_\mathrm{d}} \ll 1 \tag{7}$$

Here we demonstrate that this equivalence for $\varepsilon \ll 1$ breaks down with increasing ε. This is because a finite mean step length $\overline{r}$ in and of itself implies non-locality, regardless of whether or not the probabilistic distribution of particle step length $f_s(r)$ is thin- or heavy-tailed. A further degree of non-locality can be introduced by adopting a heavy-tailed distribution for $f_s(r)$.

ESURFD

1, 1097–1126, 2013

The standard thin-tailed form for the particle step length probability density function is the exponential distribution (e.g. Nakagawa and Tsujimoto, 1980; Hill et al., 2010):

$$f_s(r) = \frac{1}{\bar{r}} \exp\left(-\frac{r}{\bar{r}}\right) \tag{8}$$

The heavy-tailed Pareto distribution with a shift, which ensures that the maximum value of the distribution is realized at $r = 0$, can be considered as an alternative:

$$f_s(r) = \frac{\alpha r_0^\alpha}{(r + r_0)^{\alpha+1}}, \begin{cases} r_0 > 0 \\ \alpha > 0 \end{cases} \tag{9}$$

where α is the shape parameter and r_0 [L] is the scale parameter. The mean value $\bar{r}$ of the distribution of Eq. (9) can be written as:

$$\bar{r} = \frac{\alpha r_0}{\alpha - 1} - r_0, \begin{cases} r_0 > 0 \\ \alpha > 0 \end{cases} \tag{10}$$

2.2 Numerical model

Here we solve the flux and entrainment formulations under parallel conditions, the only exception being the formulation for step length. To simplify the problem and focus on this point, we approximate the flow as obeying the normal (steady, uniform) approximation. Momentum conservation then dictates that bed shear stress τ_b [$\mathrm{M\,L^{-1}\,T^{-2}}$] can be represented as proportional to the product of depth H [L] and slope S [1]:

$$\tau_\mathrm{b} = \rho u_*^2 = \rho g H S \tag{11a}$$

$$S = -\frac{\partial \eta}{\partial x} \tag{11b}$$

where u_* [$\mathrm{L\,T^{-1}}$] is the shear velocity.

ESURFD
1, 1097–1126, 2013

The dimensionless Shields number governing particle mobility is defined as

$$\tau^* = \frac{\tau_b}{\rho R g D_c} \tag{12}$$

where ρ [$\mathrm{M\,L^{-3}}$] is water density, D_c [L] is characteristic bed grain size (here taken to be uniform for simplicity) and R denotes the submerged specific gravity of the sediment (~ 1.65 for quartz).

The flow can be computed by introducing the Manning–Strickler resistance relation:

$$\frac{U}{u^*} = \alpha_r \left(\frac{H}{k_c}\right)^{1/6} \tag{13}$$

where U [$\mathrm{L\,T^{-1}}$] is the depth-averaged flow velocity, α_r is a dimensionless coefficient between 8 and 9 (Chaudhry, 1993), and k_c denotes a composite roughness height. In absence of bedforms, k_c is equivalent to the roughness height k_s which is proportional to grain size D_c by means of a dimensionless coefficient with typical values between 2 and 5 (Parker, 2004). Here, α_r is set equal to 8.1, as suggested by Parker (1991) for gravel-bed streams, while k_c, in absence of bedforms, is taken to be 2.5 times the grain size D_c (Parker, 2004).

The equation for water conservation for quasi-steady flow is:

$$Q_w = UBH \tag{14}$$

where Q_w [$\mathrm{L^3\,T^{-1}}$] is the water discharge and B [L] denotes the channel width.

Combining Eqs. (11)–(14), we relate the dimensionless Shields number to the flow properties:

$$\tau^* = \left[\frac{(k_c)^{1/3} Q_w^2}{\alpha_r^2 g B^2}\right]^{3/10} \frac{S^{7/10}}{R D_c} \tag{15}$$

ESURFD

1, 1097–1126, 2013

Morphodynamics of river bed variation with variable bedload step length

A. Pelosi and G. Parker

The basis for our morphodynamic calculations is the form of Meyer-Peter and Müller (1948), as modified by Wong and Parker (2006). It takes the form:

$$q = \gamma\sqrt{RgD_c}D_c\left(\tau^* - \tau_c^*\right)^{3/2} \tag{16}$$

where g [LT^{-2}] denotes the gravitational acceleration. The parameter τ_c^* denotes the threshold Shields number and γ is a coefficient of proportionality; these parameters take the respective values 0.0495 and 3.97 (as specified by Wong and Parker, 2006).

The volume bedload transport rate per unit width q at equilibrium can also be written as:

$$q = E \cdot \overline{r} \tag{17}$$

(Einstein, 1950), so that the entrainment rate takes the form:

$$E = \frac{\gamma}{\beta}\sqrt{RgD_c}\left(\tau^* - \tau_c^*\right)^{3/2}, \quad \beta = \frac{\overline{r}}{D_c} \tag{18}$$

Here β is a dimensionless parameter. Einstein (1950), suggested, based on a simple flume-like configuration, that $\overline{r}/D_c$ takes a value on the order of 100–1000, so that a step length is about 100–1000 grain sizes. This order of magnitude has been confirmed by the experiments of Nakagawa and Tsujimoto (1980), Wong et al. (2007) and Hill et al. (2010).

In systems with higher degrees of complexity, however, β is likely to vary over a wide range. Combinations of multiple grain sizes, bedforms, scour and fill and partially exposed bedrock are likely to give rise to connected pathways along which particles may travel for an extended distance, so giving rise to larger values of $\overline{r}$ (e.g. Parker, 2008). In order to capture this effect in a simplified 1-D model, we allow the ratio $\overline{r}$, and thus $\beta = \overline{r}/L_d$ to vary freely, so that the ratio $\overline{r}/L_d$ of step length to domain length can vary from 0 (in which case the flux and entrainment formulations become equivalent) to unity

ESURFD

1, 1097–1126, 2013

(in which a particle starting at the upstream end of the domain reaches the downstream end in a single step).

Linking Eqs. (16)–(18), the following relation arises at equilibrium conditions:

$$\frac{q}{\sqrt{RgD_c}D_c} = \beta\frac{E}{\sqrt{RgD_c}} \tag{19}$$

Our formulation is such that increased step length is adjusted against reduced entrainment, so that the equilibrium bedload transport rate is the same whether the flux or entrainment formulation is used. A difference, however, arises under disequilibrium conditions, in which case Eq. (16) is solved in conjunction with Eq. (1) in the flux case, and Eq. (18) is solved in conjunction with Eq. (4) in the entrainment case. This allows us to capture the difference between the two formulations in a comparable way.

The flux formulation, Eq. (1) corresponds to a nonlinear diffusion equation, i.e.

$$\frac{\partial\eta(x,t)}{\partial t} = \frac{\partial}{\partial x}\left(\nu\frac{\partial\eta}{\partial x}\right) \tag{20}$$

where according to Eqs. (11), (15) and (16), the kinematic diffusivity ν is a function of bed slope $S = -\partial\eta/\partial x$:

$$\nu = \frac{\sqrt{RgD_c}D_c}{S}\gamma\left\{\left[\frac{(k_c)^{1/3}Q_w^2}{\alpha_r^2 gB^2}\right]^{3/10}\frac{S^{7/10}}{RD_c} - \tau_c^*\right\}^{3/2} \tag{21}$$

The governing equation is second order in x, and thus requires two boundary conditions. Here we require that the bed elevation at the downstream end is zero, and that the sediment transport rate at the upstream end is given as a constant, specified feed rate:

$$\eta|_{x=L_d} = 0, \tag{22a}$$

$$q|_{x=0} = q_f \tag{22b}$$

ESURFD

1, 1097–1126, 2013

Morphodynamics of river bed variation with variable bedload step length

A. Pelosi and G. Parker

The entrainment formulation of Eq. (4), however, is only first order in x, in so far as the entrainment rate E is a specified function of bed slope $S = -\partial\eta/\partial x$ according to Eqs. (4) and (18). Thus there can be only one boundary condition in x; here we use Eq. (22a) for this, so that both the flux and entrainment formulations satisfy the condition of vanishing bed elevation (corresponding to set base level) at the downstream end.

Although no boundary condition can be set at the upstream end for the entrainment formulation, it is still possible to choose conditions so that the sediment transport rate at the upstream equals the feed value under equilibrium conditions.

To do this, we assume that the entrainment rate everywhere upstream of $x = 0$ equals a specified value E_f, specified as follows:

$$E_\mathrm{f} = \frac{q_\mathrm{f}}{\bar{r}} \tag{23}$$

The deposition rate $D(x)$ of Eq. (3) can then be re-written in terms of the sum of particles that originate within the domain (x–$r \geq 0$) and those that originate upstream of the domain (x–$r < 0$):

$$\begin{aligned} D(x) &= \int_0^\infty E(x-r) f_s(r)\mathrm{d}r = \int_0^x E(x-r) f_s(r)\mathrm{d}r + \int_x^\infty E(x-r) f_s(r)\mathrm{d}r \\ &= \int_0^x E(x-r) f_s(r)\mathrm{d}r + E_\mathrm{f} f_\mathrm{ls}(x) \end{aligned} \tag{24}$$

where

$$f_\mathrm{ls}(x) = \int_x^\infty f_s(r)\mathrm{d}r \tag{25}$$

ESURFD
1, 1097–1126, 2013

Morphodynamics of river bed variation with variable bedload step length

A. Pelosi and G. Parker

is the probability, that a particle travels at least a distance x [L^{-1}].

The entrainment form of sediment mass conservation thus takes the ultimate form:

$$\frac{\partial \eta}{\partial t} = -E(x) + \int_0^x E(x-r) f_s(r) \mathrm{d}r + E_\mathrm{f} f_\mathrm{ls}(x) \tag{26}$$

For the numerical computation, we non-dimensionalize Eqs. (1) and (26). We assume that the computation begins from some equilibrium initial condition with spatially constant slope S_in, bedload transport rate and entrainment rate $q_\mathrm{in} = \overline{r} E_\mathrm{in}$. At $t = 0$, however, the supply of sediment is impulsively altered, causing subsequent bed aggradation or degradation, but with an altered sediment feed rate for $t > 0$. We normalize against initial equilibrium conditions using the following definitions:

$$\hat{\eta} = \frac{\eta}{L_\mathrm{d} \cdot S_\mathrm{in}}, \tag{27a}$$

$$\hat{x} = \frac{x}{L_\mathrm{d}}, \tag{27b}$$

$$\hat{r} = \frac{r}{L_\mathrm{d}}, \tag{27c}$$

$$\hat{t} = \frac{E_\mathrm{in} \cdot \varepsilon}{L_\mathrm{d} \cdot S_\mathrm{in}} t, \tag{27d}$$

$$\hat{s} = \frac{S}{S_\mathrm{in}} \tag{27e}$$

In addition, we non-dimensionalize the entrainment rate (for the entrainment formulation) and the bedload transport rate (for the flux formulation) as

$$\hat{E} = \frac{E}{E_\mathrm{in}}, \quad \hat{q} = \varepsilon \cdot \hat{E} \tag{27f}$$

Discussion Paper | Discussion Paper | Discussion Paper | Discussion Paper |

ESURFD

1, 1097–1126, 2013

Morphodynamics of river bed variation with variable bedload step length

A. Pelosi and G. Parker

Then, the non-dimensional flux and entrainment forms of the sediment mass conservation, Eqs. (1) and (26) take the respective forms:

$$\frac{\partial \hat{\eta}}{\partial \hat{t}} = -\frac{1}{\varepsilon}\frac{\partial \hat{q}}{\partial \hat{x}} = -\frac{\partial \hat{E}}{\partial \hat{x}} \tag{28}$$

$$\frac{\partial \hat{\eta}}{\partial \hat{t}} = -\frac{1}{\varepsilon}\hat{E}(x) + \frac{1}{\varepsilon}\int_0^{\hat{x}} \hat{E}(\hat{x}-\hat{r})\tilde{f}_s\left(\frac{\hat{r}}{\varepsilon}\right)\mathrm{d}\hat{r} + \frac{1}{\varepsilon}\int_{\hat{x}}^{\infty} \tilde{f}_s\left(\frac{\hat{r}}{\varepsilon}\right)\mathrm{d}\hat{r} \tag{29}$$

where

$$\tilde{f}_s\left(\frac{\hat{r}}{\varepsilon}\right) = \frac{1}{\varepsilon}\exp\left(\frac{\hat{r}}{\varepsilon}\right) \tag{30}$$

is the dimensionless step length pdf for the exponential distribution, and

$$\tilde{f}_s\left(\frac{\hat{r}}{\varepsilon}\right) = \frac{\alpha \hat{r}_0^{\alpha}}{(\hat{r}+\hat{r}_0)^{\alpha+1}} \tag{31}$$

is the corresponding form for the Pareto distribution, where $\hat{r}_0$ is the dimensionless scale parameter equal to r_0/L_{d}.

These are the upstream conditions, for the entrainment formulation

$$\hat{E}(x,t)\Big|_{\hat{x}\le 0} = \hat{E}_{\mathrm{f}} \tag{32a}$$

and for the flux formulation

$$\hat{q}(x,t)|_{\hat{x}\le 0} = \varepsilon \hat{E}_{\mathrm{f}} \tag{32b}$$

ESURFD
1, 1097–1126, 2013

The downstream boundary condition is the same for both

$$\hat{\eta}(x,t)|_{\hat{x}=1} = 0 \tag{32c}$$

Here $\hat{E}_\mathrm{f}$ is an imposed upstream entrainment rate, and $\varepsilon\hat{E}_\mathrm{f}$ is an imposed upstream bedload feed rate, chosen to be different from the initial equilibrium values so that the bed is forced to aggrade (or degrade) toward a new equilibrium state.

Manipulating the relations Eqs. (15) and (18), with the definitions of Eq. (27), $\hat{E}$, can be at any given time as:

$$\hat{E} = \left(\frac{\tau_\mathrm{in}^*\hat{s}^{7/10} - \tau_\mathrm{c}^*}{\tau_\mathrm{in}^* - \tau_\mathrm{c}^*}\right)^{3/2} \tag{33}$$

where τ_in^* is the dimensionless Shields number, calculated from Eq. (15) with the initial flow and bed conditions and $\hat{s}$ is the local dimensionless slope.

The key parameter of interest here in describing the difference between the entrainment and flux formulations is ε. In the case $\varepsilon \ll 1$, both formulations become identical. We show below, however, that as ε increases, the response to change in sediment supply differs between the two cases.

We discretize the relation between dimensionless slope and dimensionless bed elevation as follows:

$$\hat{s} = \begin{cases} \frac{\hat{\eta}_1 - \hat{\eta}_2}{\Delta\hat{x}}, & i = 1 \\ \frac{\hat{\eta}_{i-1} - \hat{\eta}_{i+1}}{2\Delta\hat{x}}, & i = 2\ldots M \\ \frac{\hat{\eta}_M - \hat{\eta}_{M+1}}{\Delta\hat{x}}, & i = M+1 \end{cases} \tag{34}$$

The discretization of the domain is schematized in Fig. 1: a central finite-difference scheme is used to solve Eqs. (28) and (29).

ESURFD
1, 1097–1126, 2013

3 Results

Here we compare the results for aggradation and degradation for the entrainment formulation with varying values of ε against those for the flux formulation. In Fig. 2, bed elevation profiles are shown, having set as an upstream boundary condition $\hat{E}_f = 2$, so forcing the bed to aggrade. Case (a) is the solution for the flux form of Eq. (28), while cases (b), (c) and (d) are the solutions for the entrainment form of Eq. (29), solved, respectively for $\varepsilon = 0.01$, 0.5, and 1.

As expected, the solutions of Eqs. (28) and (29) collapse to the same results in the case of $\varepsilon = 0.01$, i.e. when the mean particle step length is short compared to the length of the domain. Thus under this condition the local (flux) form, essentially coincides with the non-local form. For higher values of ε, however, the differences between the results increase because the entrainment form is able to capture the non-local feature of the particle movement. For the flux form and the case $\varepsilon = 0.01$, the aggradational profile is strongly upward concave, with bed slop declining downstream. The transient aggradational bed profiles tend to assume a nearly linear profile, and thus the bed rotates upward, for values of ε close to 0.5. For higher values a downward-concave form profile is realized.

To highlight and quantify this change in shape, we introduce a concavity parameter δ, which measures the deviation, in the centre of the profile, at $\hat{x} = 0.5$ relative to thea constant initial slope:

$$\delta = \frac{0.5 \cdot \hat{\eta}|_{\hat{x}=0} - \hat{\eta}|_{\hat{x}=0.5}}{\hat{\eta}|_{\hat{x}=0}} \tag{35}$$

where $\hat{\eta}|_{\hat{x}=0}$ denotes the dimensionless bed elevation at $\hat{x} = 0$ and $\hat{\eta}|_{\hat{x}=0.5}$ denotes the same quantity in the center of the profile ($\hat{x} = 0.5$). Positive δ indicates upward concavity, while negative δ indicates downward concavity. In Fig. 3, the variation in time of δ is shown for the flux case, and different values of ε for the entrainment case. It is seen that δ is positive for smaller ε and but becomes negative for ε greater than 0.5. The results for the flux form overlap with the form for $\varepsilon = 0.01$.

ESURFD
1, 1097–1126, 2013

In Fig. 4, the slope evolution is plotted: the typical upward concave shape for the flux case and $\varepsilon = 0.01$ is due to the preferential proximal deposition of sediment, which causes the sediment load, and thus the Shields number τ^* to decrease downstream (Parker, 2004). Thus, according to Eq. (15), a downstream decreasing slope is realized (Fig. 4a and b). On the other hand, a downward concave shape for $\varepsilon = 1$ is characterized by an increasing slope downstream (Fig. 4d). This corresponds to bedload particles that can jump from the upstream end of the domain to the downstream end in one step.

For completeness, the case of degradation, due to an imposed entrainment and feed rate upstream $\hat{E}_\mathrm{f} = 1/2$, is described by Figs. 5–7. The results show a congruent behavior with the aggradation case. In Fig. 5, for $\varepsilon = 0.01$ and $\hat{E}_\mathrm{f} = 1/2$, it is seen that the two profiles more or less agree. In Fig. 6, the concavity parameters δ also more or less agree for this case. When ε increases to 1, the concavity of the transient degradational profiles changes from downward to upward. In Fig. 7, slope changes from increasing downstream to decreasing upstream. When $\varepsilon = 0.5$, it is shown in Fig. 7 that the transient profile tend to keep a straight shape, and the evolution of the bed is essentially rotational about the downstream end.

Summarizing (i) the flux model and the entrainment model yield essentially the same results for $\varepsilon = 0.01$; (ii) for $\varepsilon = 0.5$, nearly rotational aggradation and degradation are obtained; and (iii) for $\varepsilon = 1$, the pattern of concavity is reversed compared to the flux case.

Then, a Pareto distribution with a shift, i.e. Eq. (9) for particle step length distribution is considered as well, so as to compare the case of heavy tail of the pdf of step length with the thin-tail exponential form. In the calculations for the entrainment rate with $\hat{E}_\mathrm{f} = 2$, two cases are evaluated, (a) $\varepsilon = 0.015$ and (b) $\varepsilon = 1$. It is seen that the two profiles more or less agree for the case (a). A more substantial difference is seen for case (b), but the concavity is quite small for both the cases of thin-tailed and heavy-tailed pdf for step length. Assuming $L = 200$ m, with a thin-tailed pdf the value $\varepsilon = 0.015$ corresponds to a mean step length equal to 3 m, and the value $\varepsilon = 1$ corresponds to 200 m. We have

ESURFD

1, 1097–1126, 2013

Morphodynamics of river bed variation with variable bedload step length

A. Pelosi and G. Parker

set the shape parameter α is in the Pareto pdf equal to 1.5, and the scale parameter r_0 equal to 1.5 m for case (a), and t100 m for case (b). This yields values of $\bar{r}$ from Eq. (10), that are respectively equal to 3 m and 200 m, i.e. the same values as the thin-tailed case.

The analysis shows that the shape of the tail of the step length pdf does not significantly change the results for $\varepsilon = 0.015$ but does result in some change compared to the thin-tailed case $\varepsilon = 1$. Figure 8 shows the long profiles resulting from both the thin-tailed and heavy-tailed case, and Fig. 9 shows the corresponding evolution of concavity. As seen from Fig. 9c and d corresponding to the case of aggradation with $\varepsilon = 1$, the profiles are downward-concave for the thin-tailed pdf of step length, and upward-concave for the heavy-tailed case. The concavity in both cases, however, is so small that the same rotational behavior for profile adjustment is seen, as documented in Fig. 8c and d.

4 Discussion and conclusions

The main goal of the work is to show how the entrainment form of the Exner equation of sediment continuity diverges from the flux form of the Exner equation when non-local behavior in particle motion arises: (i) as the mean particle step length $\bar{r}$ increases from 0 to the order of magnitude of the domain length L_d for a thin-tailed step length pdf and (ii) as a heavy-tailed pdf for particle step length is used.

The dimensionless parameter ε is defined as the ratio between the mean step length $\bar{r}$ and the length of the domain of interest L_d. We analyzed the effect of variation of ε on bed aggradational/degradational profiles by solving the entrainment form of the Exner equation, with the assumption of thin-tailed pdf for particle step length. As expected, the two forms collapse in the case $\varepsilon \ll 1$.

For high values of ε, however, the differences between the results from the two forms increase because of the non-locality of particle movement which is not captured by the classical flux form of the Exner equation: the transient aggradational (degradational)

ESURFD
1, 1097–1126, 2013

bed profiles tend to assume, for ε greater than 0.5, a downward (upward) concave shape, rather than the upward (downward) concave shape of the flux form. When the value of ε is close to 0.5, an interesting behavior for both the cases of aggradation and degradation has been found: the transient profiles tend to rotate around the downstream point, keeping almost a straight shape. For value of ε in the range $[0, 0.5)$, the concavity of the bed profiles is still upward for aggradation and downward, for degradation, but by increasing ε to 0.5, the concavity is nearly vanishing. These results may serve as an explanation for relatively flat aggradational bed profiles which have been achieved in some short laboratory experiments (e.g. Muto, 2001; Voller and Paola, 2010), where the value of the ratio between mean particle step length and length of the domain of interest may not be negligible. At the laboratory scale, the mean step length becomes comparable to domain length so that the inclusion ofnon-local effects in the pdf of step length which this circumstance entails, should clearly be evaluated in order to properly model the bed evolution.

The analysis also investigates the effect of the heavy tailedness in the pdf of step length on bed profile. For the case studied, we show that the variation of the shape of the step length distribution from thin- to heavy-tailed does not significantly influence the results when step length is small. This is probably due to the "short" domain length compared to the tail of the power law distribution. There is a somewhat larger difference in the case when step length equals domain length, but the bed elevation profiles are nearly linear for both thin-tailed and heavy-tailed pdf. Voller and Paola (2010) introduced heavy-tailed behavior to explain profiles that evolve with concavity that is small compared to the standard flux case of Eq. (1). Here we find that a heavy-tailed behavior is not necessary to obtain this result.

Long step lengths of bedload particles in the field may result from any bed pattern that induces preferential paths for transport, including grain size mixtures (Ganti et al., 2010), bedforms, scour and fill, and intermittent bedrock exposure (Stark et al., 2009). Thus our results may be applicable to these cases. The case of sediment suspension can also be represented in entrainment form (e.g. Parker, 2004). This case is generally

ESURFD
1, 1097–1126, 2013

associated with much longer mean path lengths than the case of bedload. As a result, the suspension-dominated case may show much more non-local behavior than the bedload case. This case deserves further investigation.

Acknowledgements. Anna Pelosi was supported by the Ph.D in Civil and Environmental Engineering program of the University of Salerno and hosted by the CEE Department of the University of Illinois at Urbana-Champaign. This research was motivated in part by a comment from D. Jerolmack.

References

Bradley, D. N., Tucker, G. E., and Benson, D. A.: Fractional dispersion in a sand bed river, J. Geophys. Res., 115, F00A09, doi:10.1029/2009JF001268, 2010.

Chaudhry, M. H.: Open-Channel Flow, Prentice-Hall, Englewood Cliffs, 483 pp., 1993.

Einstein, H. A.: The Bed-load Function for Sediment Transportation in Open Channel Flows, Technical Bulletin 1026, US Dept. of the Army, Soil Conservation Service, Washington, D. C., 1950.

Exner, F. M.: Zur Physik der Dünen, Akad. Wiss. Wien Math. Naturwiss. Klasse, 129, 929–952, 1920.

Exner, F. M.: Über die Wechselwirkung zwischen Wasser und Geschiebe in Flüssen, Akad. Wiss. Wien Math. Naturwiss. Klasse, 134, 165–204, 1925.

Foufoula-Georgiou, E., Ganti, V., and Dietrich, W.: A nonlocal theory of sediment transport on hillslopes, J. Geophys. Res., 115, F00A16, doi:10.1029/2009JF001280, 2010.

Ganti, V., Meerschaert, M. M., Foufoula-Georgiou, E., Viparelli, E., and Parker, G.: Normal and anomalous diffusion of gravel tracer particles in rivers, J. Geophys. Res., 115, F00A12, doi:10.1029/2008JF001222, 2010.

Hassan, M. A., Voepel, H., Schumer, R., Parker, G., and Fraccarollo, L.: Displacement characteristics of coarse fluvial bed sediment, J. Geophys. Res.-Earth Surf., 118, 155–165, doi:10.1029/2012JF002374, 2013.

Hill, K. M., DellAngelo, L., and Meerschaert, M. M.: Heavy-tailed travel distance in gravel bed transport: An exploratory enquiry, J. Geophys. Res., 115, F00A14, doi:10.1029/2009JF001276, 2010.

ESURFD

1, 1097–1126, 2013

Martin, R. L., Jerolmack, D. J., and Schumer, R.: The physical basis for anomalous diffusion in bed load transport, J. Geophys. Res., 117, F01018, doi:10.1029/2011JF002075, 2012.
Meyer-Peter, E. and Müller, R.: Formulas for bed-load transport, in: Proceedings of the 2nd Congress of the International Association of Hydraulic Research, Stockholm, 39–64, 1948.
Muto, T.: Shoreline autoretreat substantiated in flume experiment, J. Sediment Res., 71, 246–254, 2001.
Nakagawa, H. and Tsujimoto, T.: A stochastic model for bed load transport and its applications to alluvial phenomena, in: Application of Stochastic Processes in Sediment Transport, edited by: Shen, H. W. and Kikkawa, H., Water Resources Publications, Colorado, USA, 1980.
Nikora, V., Habersack, H., Huber, T., and McEwan, I.: On bed particle diffusion in gravel bed flows under weak bed load transport, Water Resour. Res., 38, 1081, doi:10.1029/2001WR000513, 2002.
Paola, C. and Voller, V. R.: A generalized Exner equation for sediment mass balance, J. Geophys. Res., 110, F04014, doi:10.1029/2004JF000274, 2005.
Paola, C., Heller, P. L., and Angevine, C. L.: The largescale dynamics of grain-size variation in alluvial basins, 1: Theory, Basin Res., 4, 73–90, 1992.
Parker, G.: Selective sorting and abrasion of river gravel, II: Applications, J. Hydraul. Eng., 117, 150–171, 1991.
Parker, G.: 1D Sediment Transport Morphodynamics with Applications to Rivers and Turbidity Currents, Copyrighted e-book, available at: http://hydrolab.illinois.edu/people/parkerg//morphodynamics_e-book.htm, 2004.
Parker, G.: Transport of gravel and sediment mixtures, in: Sedimentation Engineering Processes, Measurements, Modeling and Practice, edited by: Garcia, M., ASCE Manual and Reports on Engineering Practice, 110, Am. Soc. of Civ. Eng., New York, chap. 3, 165–252, 2008.
Parker, G., Paola, C., Whipple, K., and Mohrig, D.: Alluvial fans formed by channelized fluvial and sheet flow, I: Theory, J. Hydraul. Eng., 124, 985–995, doi:10.1061/(ASCE)0733-9429(1998)124:10(985), 1998.
Parker, G., Paola, C., and Leclair, S.: Probabilistic Exner sediment continuity equation for mixtures with no active layer, J. Hydraul. Eng., 126, 818–826, 2000.
Postma, G., Kleinhans, M. G., Meijer, P. T., and Eggenhuisen, J. T.: Sediment transport in analogue flume models compared with real world sedimentary systems: a new look

ESURFD

1, 1097–1126, 2013

Morphodynamics of river bed variation with variable bedload step length

A. Pelosi and G. Parker

at scaling sedimentary systems evolution in a flume, Sedimentology, 55, 1541–1557, doi:10.1111/j.1365-3091.2008.00956.x, 2008.

Sayre, W. and Hubbell, D.: Transport and dispersion of labeled bed material, North Loup River, Nebraska, US Geol. Surv. Prof. Pap., 433-C, 48 pp., 1965.

Schumer, R., Benson, D. A., Meerschaert, M. M., and Baeumer, B.: Fractal mobile/immobile solute transport, Water Resour. Res., 39, 1296, doi:10.1029/2003WR002141, 2003.

Schumer, R., Meerschaert, M. M., and Baeumer, B.: Fractional advection-dispersion equations for modeling transport at the Earth surface, J. Geophys. Res., 114, F00A07, doi:10.1029/2008JF001246, 2009.

Stark, C. P., Foufoula-Georgiou, E., and Ganti, V.: A nonlocal theory of sediment buffering and bedrock channel evolution, J. Geophys. Res., 114, F01029, doi:10.1029/2008JF000981, 2009.

Tsujimoto, T.: Probabilistic model of the process of bed load transport and its application to mobile-bed problems, Ph. D. thesis, Kyoto Univ., Kyoto, Japan, 174 pp., 1978.

Voller, V. R. and Paola, C.: Can anomalous diffusion describe depositional fluvial profiles?, J. Geophys. Res., 115, F00A13, doi:10.1029/2009JF001278, 2010.

Voller, V. R., Ganti, V., Paola, C., and Foufoula-Georgiou, E.: Does the flow of information in a landscape have direction?, Geophys. Res. Lett., 39, L01403, doi:10.1029/2011GL050265, 2012.

Whipple, K. X., Parker, G., Paola, C., and Mohrig, D.: Channel dynamics, sediment transport, and the slope of alluvial fans: experimental study, J. Geol., 106, 677–693, 1998.

Wong, M. and Parker, G.: Reanalysis and correction of bed-load relation of Meyer-Peter and Müller using their own database, J. Hydraul. Eng., 132, 1159–1168, 2006.

Wong, M., Parker, G., DeVries, P., Brown, T. M., and Burges, S. J.: Experiments on dispersion of tracer stones under lower-regime plane-bed equilibrium bed load transport, Water Resour. Res., 43, W03440, doi:10.1029/2006WR005172, 2007.

ESURFD

1, 1097–1126, 2013

Title Page

Abstract | Introduction

Conclusions | References

Tables | Figures

◀| |▶

◀ ▶

Back | Close

Full Screen / Esc

Printer-friendly Version

Interactive Discussion

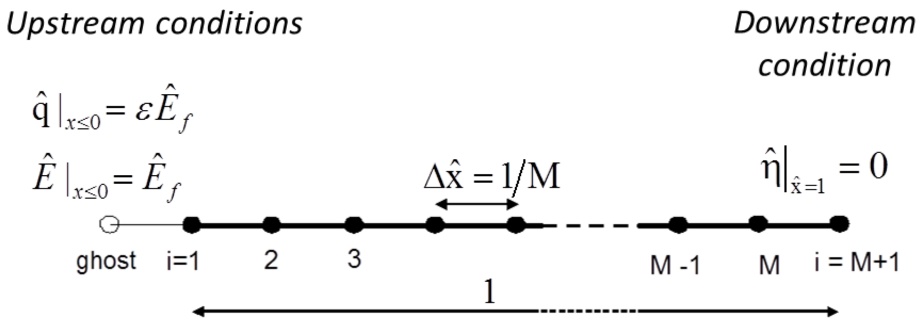

Fig. 1. Discretization of the domain.

ESURFD

1, 1097–1126, 2013

Morphodynamics of river bed variation with variable bedload step length

A. Pelosi and G. Parker

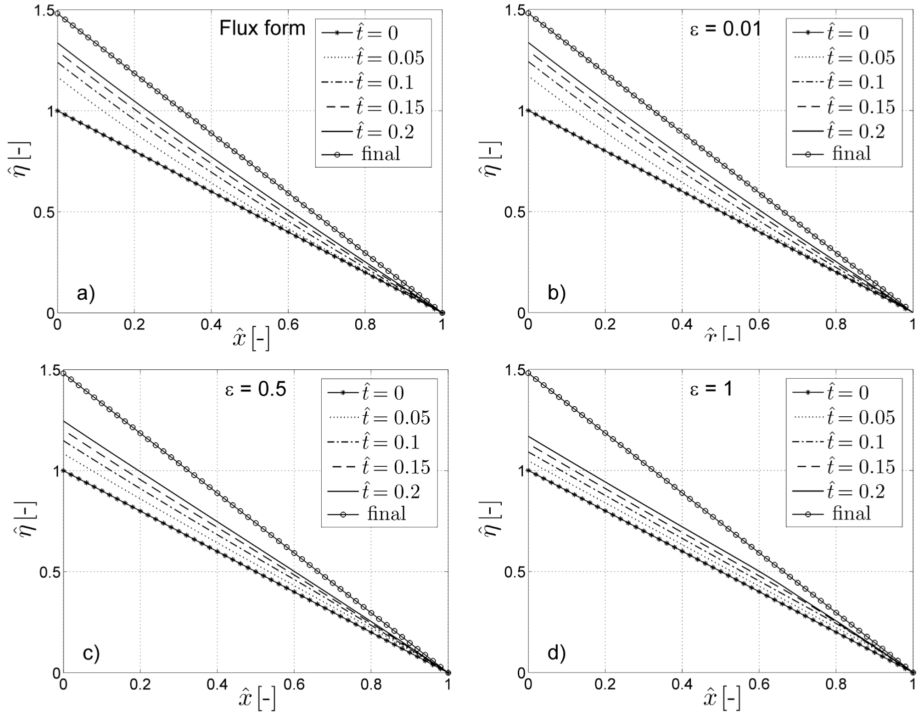

Fig. 2. Bed profile evolution for the case $\hat{E}_\mathrm{f} = 2$: **(a)** flux form; **(b)** entrainment form for $\varepsilon = \overline{r}/L_\mathrm{d} = 0.01$, **(c)** entrainment form for $\varepsilon = 0.5$ and **(d)** entrainment form for $\varepsilon = 1$, using the thin-tailed exponential step length function of Eq. (8).

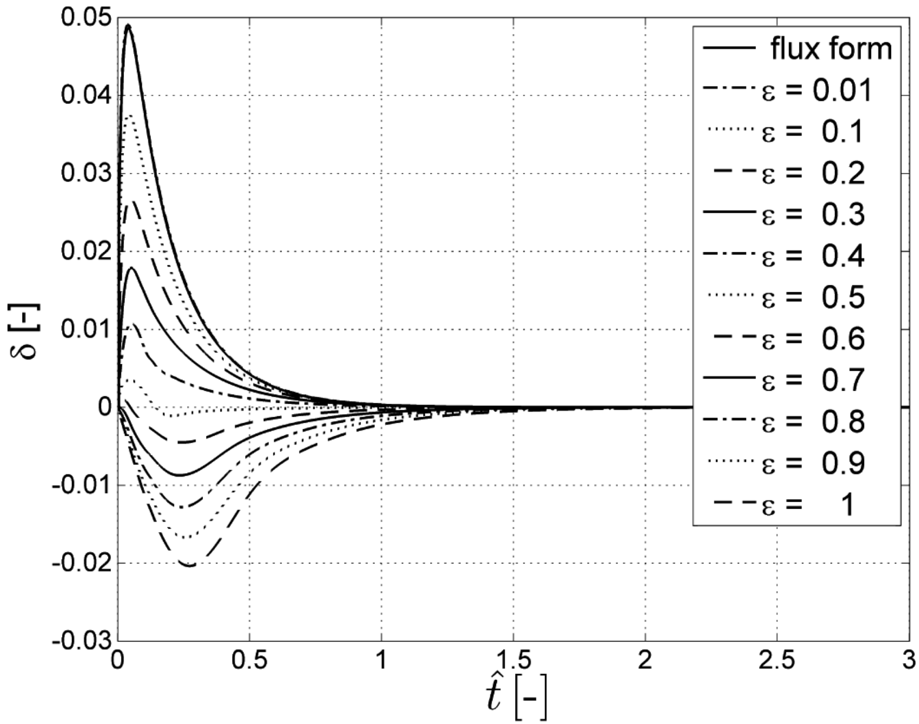

Fig. 3. Aggradation case: variation in time of the concavity parameter δ in the case of the flux formulation and in the cases of the entrainment formulation for different values of ε ranging from 0.01 to 1. The result for the flux form overlaps with the result for the entrainment form with $\varepsilon = 0.01$.

Discussion Paper | Discussion Paper | Discussion Paper | Discussion Paper |

ESURFD

1, 1097–1126, 2013

Morphodynamics of river bed variation with variable bedload step length

A. Pelosi and G. Parker

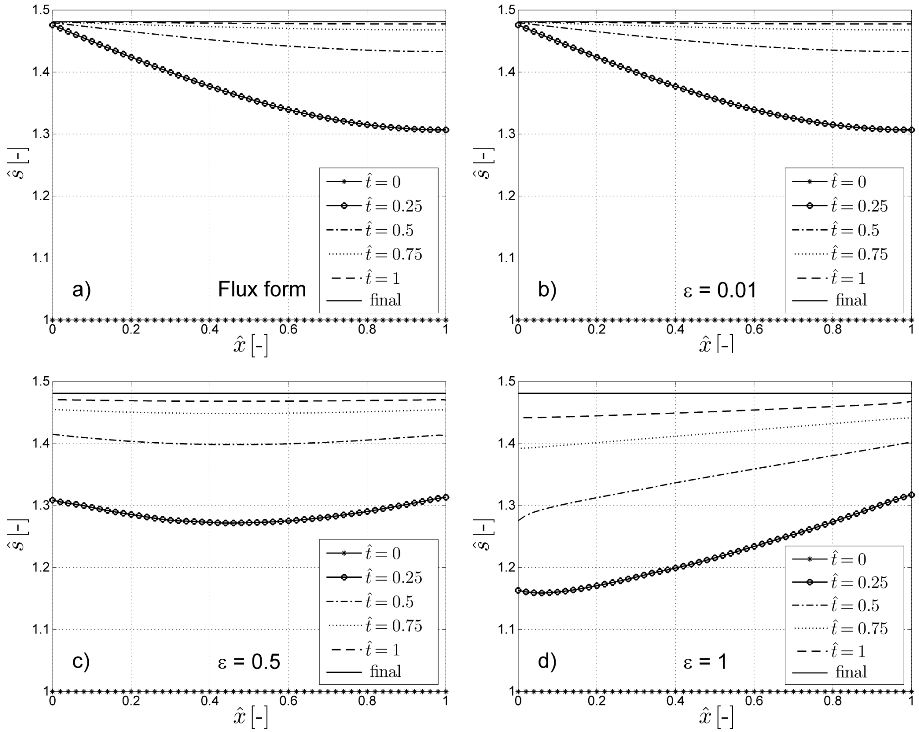

Fig. 4. Slope profile evolution for the case $\hat{E}_f = 2$: **(a)** flux form; **(b)** entrainment form for $\varepsilon = \overline{r}/L_d = 0.01$, **(c)** entrainment form for $\varepsilon = 0.5$ and **(d)** entrainment form for $\varepsilon = 1$, using the thin-tailed exponential step length function of Eq. (8).

ESURFD
1, 1097–1126, 2013

Morphodynamics of river bed variation with variable bedload step length

A. Pelosi and G. Parker

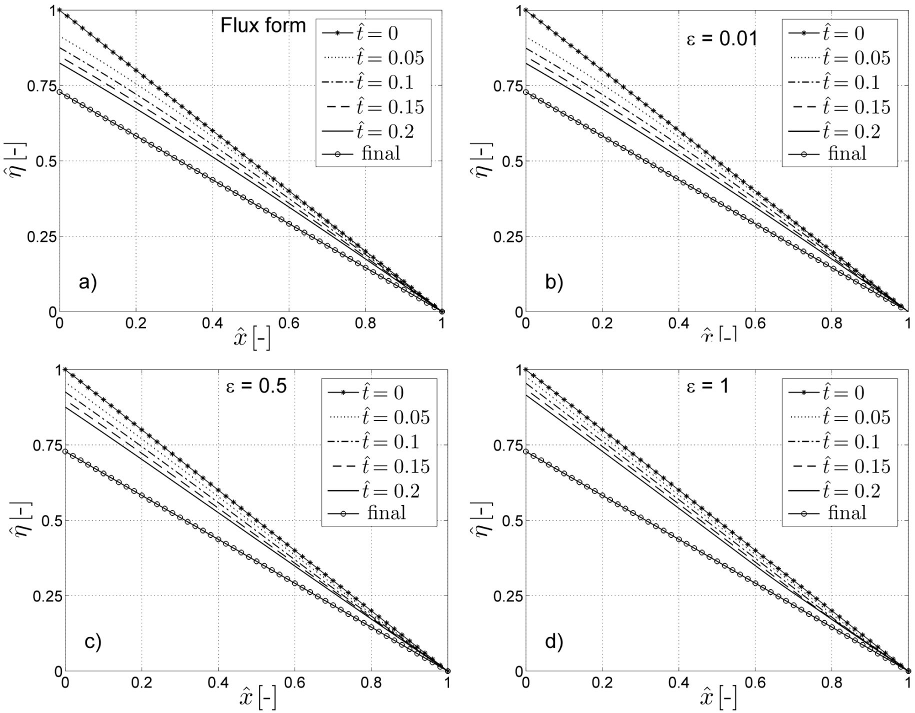

Fig. 5. Bed profile evolution for the case $\hat{E}_{\mathrm{f}} = 1/2$: **(a)** flux form; **(b)** entrainment form for $\varepsilon = \overline{r}/L_{\mathrm{d}} = 0.01$, **(c)** entrainment form for $\varepsilon = 0.5$ and **(d)** entrainment form for $\varepsilon = 1$, using the thin-tailed exponential step length function of Eq. (8).

ESURFD
1, 1097–1126, 2013

Morphodynamics of river bed variation with variable bedload step length

A. Pelosi and G. Parker

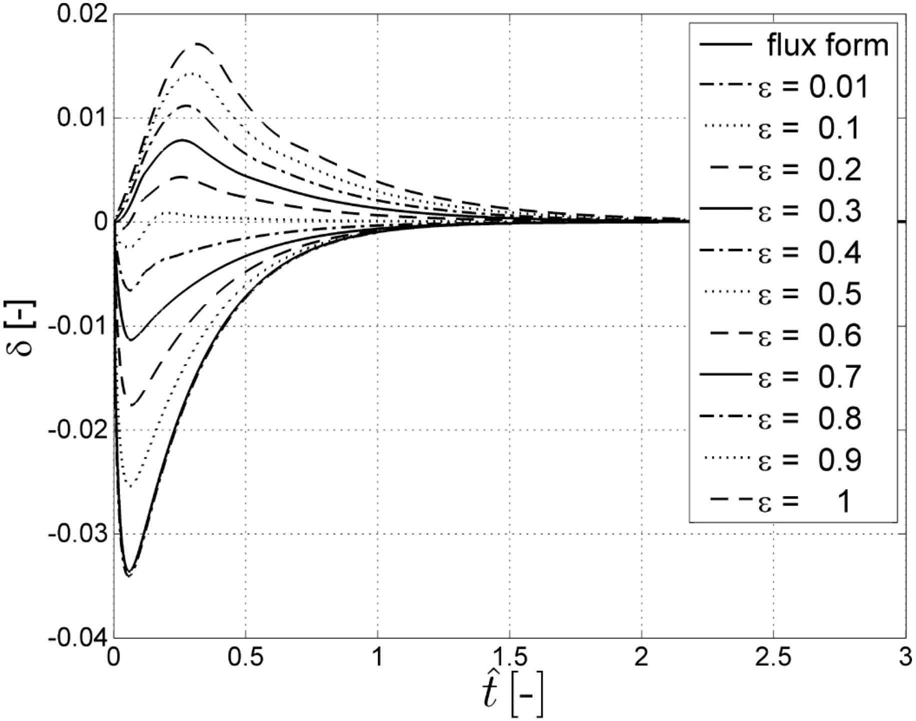

Fig. 6. Degradation case: variation in time of the concavity parameter δ in the case of the flux formulation and in the cases of the entrainment formulation for different values of ε ranging from 0.01 to 1. The result for the flux form overlaps with the result for the entrainment form with $\varepsilon = 0.01$.

ESURFD

1, 1097–1126, 2013

Morphodynamics of river bed variation with variable bedload step length

A. Pelosi and G. Parker

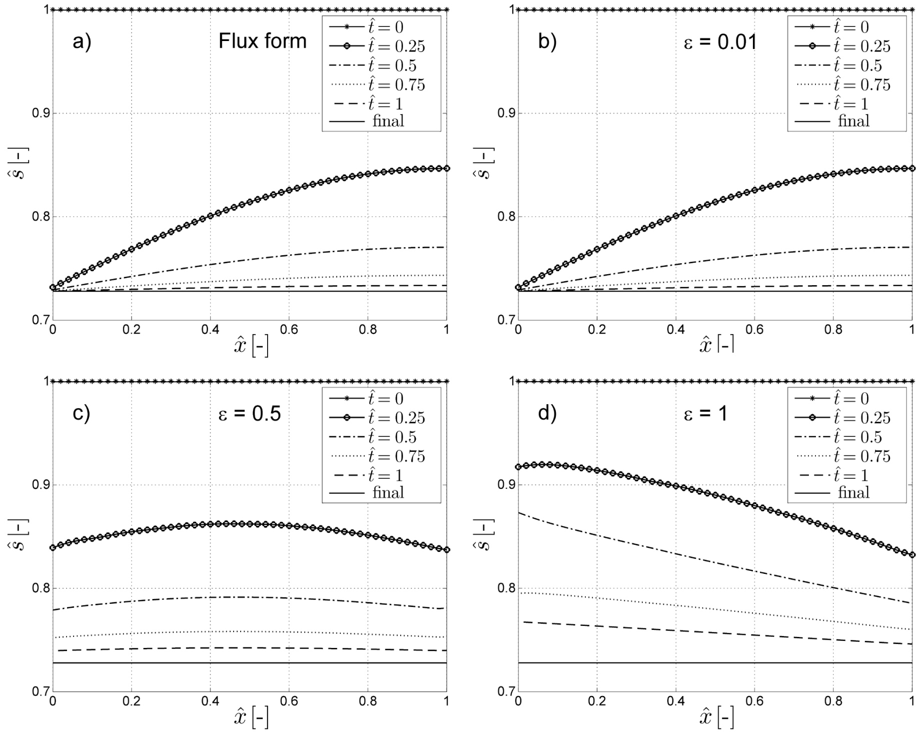

Fig. 7. Slope profile evolution for the case $\hat{E}_f = 1/2$: **(a)** flux form; **(b)** entrainment form for $\varepsilon = \overline{r}/L_d = 0.01$, **(c)** entrainment form for $\varepsilon = 0.5$ and **(d)** entrainment form for $\varepsilon = 1$, using the thin-tailed exponential step length function of Eq. (8).

ESURFD
1, 1097–1126, 2013

Morphodynamics of river bed variation with variable bedload step length

A. Pelosi and G. Parker

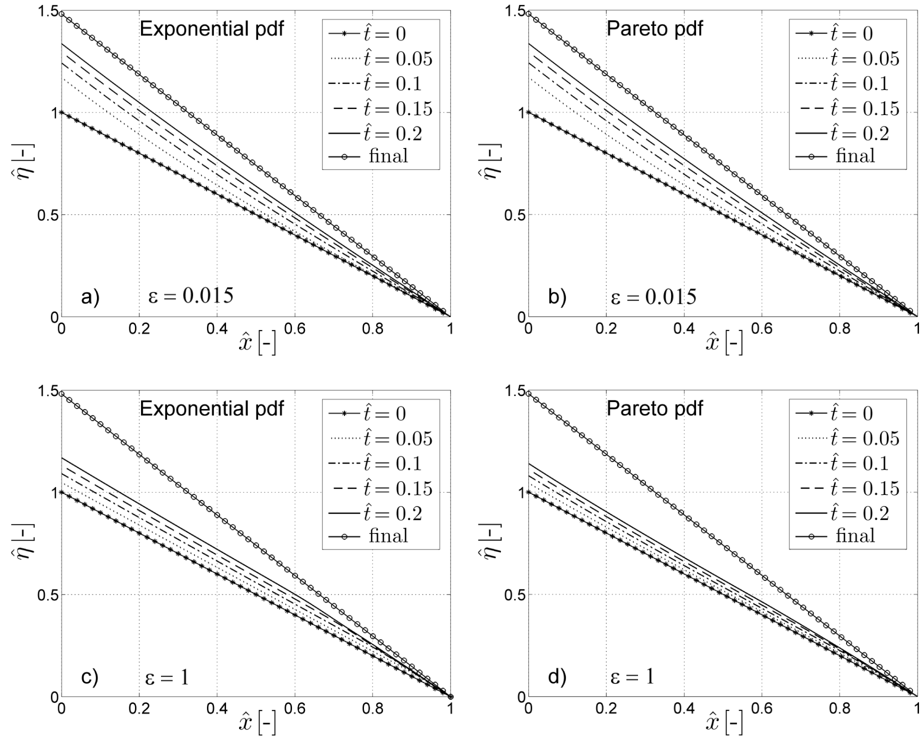

Fig. 8. Bed profile evolution for the case $\hat{E}_\mathrm{f}$ = 2. ε = 0.015: **(a)** thin-tailed exponential step length pdf; **(b)** heavy-tailed Pareto step length pdf (α = 1.5, r_0 = 1.5 m). ε = 1: **(c)** thin-tailed exponential step length pdf; **(d)** heavy-tailed Pareto step length pdf (α = 1.5, r_0 = 100 m).

ESURFD

1, 1097–1126, 2013

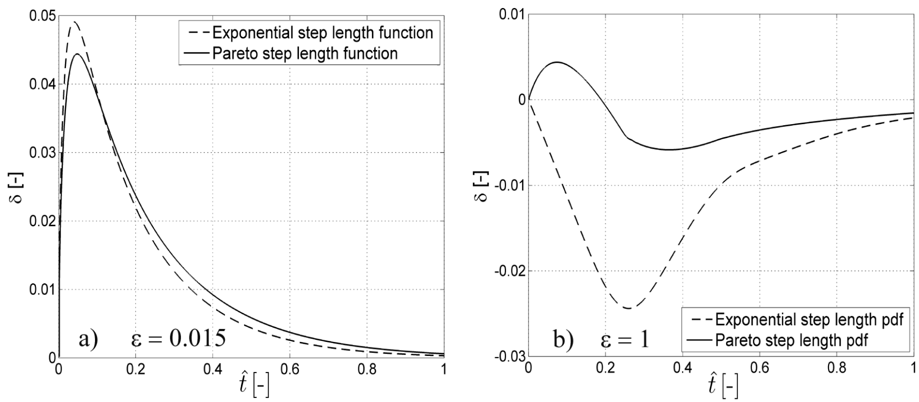

Fig. 9. Variation in time of the concavity parameter δ for the case of the thin-tailed exponential distribution for step length, and the case of heavy-tailed Pareto distribution for step length. The parameter $\varepsilon = \overline{r}/L_d$ takes the value 0.015 in **(a)** and 1.0 in **(b)**.